

## SIMULATION ANALYSIS OF A ONE-DIMENSIONAL SEDIMENTATION MODEL

Liesbeth B. Verdickt Jan F. Van Impe

*BioTeC–Bioprocess Technology and Control*  
*Katholieke Universiteit Leuven, B-3001 Leuven (Belgium)*  
Fax: +32-16-32.19.60 e-mail: jan.vanimpe@agr.kuleuven.ac.be

**Abstract:** One-dimensional models for describing the secondary settler in activated sludge wastewater treatment are important with respect to process control and optimization. The most widely used one-dimensional model nowadays is the model presented by Takács *et al.* (1991). In this paper, the model of Takács *et al.* is thoroughly studied at the simulation level. Simulations have been performed to analyze the dynamic behaviour of the concentration profile and to examine the influence on the steady state concentration profile of (i) the loading characteristics (influent concentration and flow rate), and (ii) the number of layers considered in the settler. The simulations reveal a major shortcoming of the Takács model, namely, its inconsistency with respect to the number of layers considered in the discretized equations. The identification problem resulting from this inconsistency is clearly illustrated. As an alternative, the (consistent) model of Hamilton *et al.* (1992) is proposed.

**Keywords:** biotechnology, modelling, water pollution, distributed parameter systems, simulation

### 1. INTRODUCTION

In the last few decades, many models have been presented for describing the secondary clarifier in activated sludge wastewater treatment systems, ranging from relatively simple one-dimensional models that consider only the vertical direction to two- and three-dimensional models that include complex hydrodynamics. In the field of process control and optimization, the focus is on 1D models because of their low complexity.

The usual starting point for one-dimensional modelling of the dynamics of settlers is the solids flux theory of Kynch (1952), which assumes that the settling process can be determined entirely by a continuity equation. The theory can be made operational in computer programs by splitting up the secondary settler into  $n$  horizontal layers of equal height, and by discretizing the continuity equation on these layers. A major problem of the flux theory is the fact that the continuity equation predicts a constant concentration profile to occur in the settler at steady state, which is in contradiction with experimental observations (Section 2). Several models have been proposed that overcome this difficulty. Today, the model published by Takács *et al.* (1991) is widely used. However, the detailed simulation analysis summarized in

this paper clearly illustrates the limitations of this model, in particular, the inconsistency of the model output with respect to the number of layers used in the discretized equations (see also Jeppsson and Diehl 1996). The resulting practical identification problem is highlighted (Section 3). The model of Hamilton *et al.* (1992) is put forward as an alternative, because of its ability to describe a non-constant concentration profile on which the number of layers only has a resolution effect (Section 4). Section 5 summarizes the main conclusions.

### 2. SOLIDS FLUX THEORY FUNDAMENTALS

#### 2.1 Continuity equation

The solids flux theory is based on the assumption that the settling process can be determined entirely by a continuity equation without specifying the details of the forces on the sludge particles. The simplest form of the continuity equation is

$$\frac{\partial X}{\partial t} + \frac{\partial J}{\partial z} = 0 \quad (1)$$

- $X$  : suspended solids concentration [g/m<sup>3</sup>]  
 $t$  : time [h]  
 $J$  : solids flux [g/(h · m<sup>2</sup>)]  
 $z$  : spatial coordinate in vertical direction (positive downwards) [m]

## 2.2 Total solids flux

In a secondary settler, the total solids flux  $J$  consists of the bulk ( $J_b$ ) and the settling ( $J_s$ ) flux:

$$J = J_b + J_s \quad (2)$$

The solids flux due to bulk flow is equal to

$$J_b = q \cdot X \quad (3)$$

where  $q$  is the bulk flow velocity [m/h]. Assuming a constant horizontal cross section  $A$  over the entire depth,  $q$  is only dependent on whether the observed cross section is in the underflow region (under the inlet position) or in the overflow region (above the inlet position), i.e.:

$$q = \begin{cases} q_{un} = \frac{Q_{un}}{A} & \text{in the underflow region} \\ -q_{ov} = -\frac{Q_e}{A} & \text{in the overflow region} \end{cases} \quad (4)$$

$Q_{un}$  : underflow flow rate [m<sup>3</sup>/h]  
 $Q_e$  : effluent flow rate [m<sup>3</sup>/h]

The settling (gravitational) flux equals

$$J_s = v_s \cdot X \quad (5)$$

where  $v_s$  is the settling velocity of the sludge particles [m/h]. The solids flux theory assumes that the sludge settling velocity is only dependent on the local particles concentration. The most widely used function to relate the settling velocity  $v_s$  with the solids concentration  $X$  is the exponential settling velocity function of Vesilind (1968):

$$v_s(X) = k_1 \cdot \exp(-k_2 X) \quad (6)$$

where  $k_1$  and  $k_2$  are parameters used for calibrating the function to experimental data. This settling velocity function has been developed to describe the hindered settling behaviour of particles, i.e., the settling behaviour at relatively high solids concentrations where inter-particle forces hinder the sedimentation and the mass of particles tends to settle as a unit. The function overestimates the settling velocity for low concentrations of solids (usually found in the overflow region of the settler). In order to make the basic approach of the solids flux theory applicable for low concentrations, a number of settling velocity functions have been proposed that start at zero settling velocity for very low concentrations (Takács *et al.* 1991, Dupont and Dahl 1995). The settling velocity function proposed by Takács *et al.* (1991) is a double-exponential extension of the Vesilind function:

$$v_s(X) = \max \left( 0, \min \left( v'_0, v_0 \cdot \left( e^{-r_n(X-X_{min})} - e^{-r_p(X-X_{min})} \right) \right) \right) \quad (7)$$

The function contains five model parameters:

$v_0$  and  $v'_0$  theoretical and practical maximum settling velocities [m/h]  
 $X_{min}$  suspended solids concentration below which the settling velocity equals zero [g/m<sup>3</sup>]  
 $r_h$  and  $r_p$  parameters associated with the settling behaviour in the hindered settling zone and at low solids concentrations, respectively [m<sup>3</sup>/g]

The settling velocity functions of Vesilind and Takács *et al.* are presented together in Figure 1: the function of Takács *et al.* reduces to the one of Vesilind at high concentrations.

## 2.3 Discretization

The flux theory can be made operational in computer programs by splitting up the secondary settler into  $n$  horizontal layers of equal height, and by discretizing the continuity equation on these layers. The resulting model consists of  $n$  ordinary differential equations.

· Top layer (layer 1):

$$h \cdot \frac{dX_1}{dt} = q_{ov} \cdot X_2 - q_{ov} \cdot X_1 - J_{s,1} \quad (8)$$

·  $i$ -th layer in overflow zone ( $2 \leq i \leq m-1$ ):

$$h \cdot \frac{dX_i}{dt} = q_{ov} \cdot X_{i+1} - q_{ov} \cdot X_i + J_{s,i-1} - J_{s,i} \quad (9)$$

· Feed layer (layer  $m$ ):

$$h \cdot \frac{dX_m}{dt} = \frac{Q_f}{A} \cdot X_f - q_{ov} \cdot X_m - q_{un} \cdot X_m + J_{s,m-1} - J_{s,m} \quad (10)$$

·  $i$ -th layer in underflow section ( $m+1 \leq i \leq n-1$ ):

$$h \cdot \frac{dX_i}{dt} = q_{un} \cdot X_{i-1} - q_{un} \cdot X_i + J_{s,i-1} - J_{s,i} \quad (11)$$

· Bottom layer (layer  $n$ ):

$$h \cdot \frac{dX_n}{dt} = q_{un} \cdot X_{n-1} - q_{un} \cdot X_n + J_{s,n-1} \quad (12)$$

The settling flux  $J_{s,i}$  between two adjacent layers  $i$  and  $i+1$  equals  $v_s(X_i) \cdot X_i$ . A schematic view of the discretized settler is presented in Figure 2.

## 2.4 Fundamental problem of the solids flux theory

A major problem of the solids flux theory is that at steady state the continuity equation yields a constant concentration profile (Queinnec and Dochain 2001): changes of the concentration in function of depth will only occur at the boundaries, i.e., at the inlet level and at the top and the bottom of the clarifier.

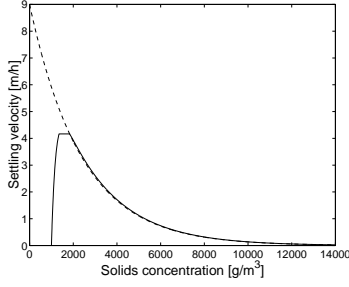


Fig. 1. Settling velocity in function of the solids concentration according to the Vesilind (dashed line) and the Takács *et al.* (solid line) settling velocity function.

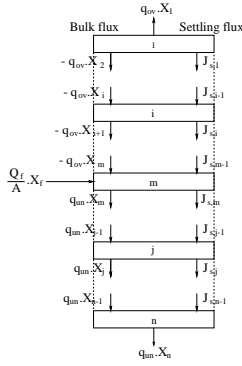


Fig. 2. Schematic view of a discretized settler.

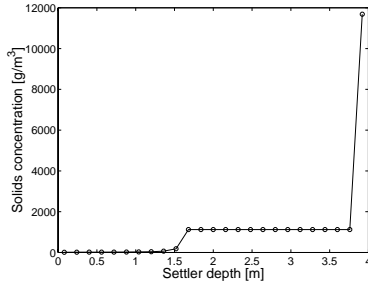


Fig. 3. Typical steady state profile obtained by discretization of the continuity equation. The settling velocity is described by Equation (7).

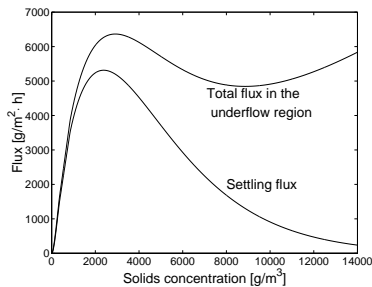


Fig. 4. Takács model: settling flux and total flux in the underflow region in function of the solids concentration.

This is illustrated in Figure 3. (Observe that the occurrence of a non-constant concentration profile in the overflow zone is due to the discretization. In this zone, the flux between two adjacent layers  $i$  and  $i + 1$  is dependent on both  $X_i$  and  $X_{i+1}$ . In the underflow region, where the flux between two layers  $i$  and  $i + 1$  is determined entirely by  $X_i$ , a constant concentration profile is obtained.) Several one-dimensional models have been proposed in literature that circumvent the difficulty of a constant steady state profile in the underflow zone. Most often, a restraint is put on the gravity flux after discretization of the continuity equation (Takács *et al.* 1991, Otterpohl and Freund 1992, Dupont and Dahl 1995).

### 3. MODEL OF TAKÁCS *ET AL.* (1991)

The model of Takács *et al.* (1991) uses balance equations (8) to (12), with the following restriction on the gravity flux from layer  $i$  to layer  $i + 1$ :

· Overflow zone ( $1 \leq i \leq m - 1$ ):

$$J_{s,i} = \min \left( v_s(X_i) \cdot X_i, v_s(X_{i+1}) \cdot X_{i+1} \right) \quad (13)$$

$$J_{s,i} = v_s(X_i) \cdot X_i \quad \text{if } X_{i+1} > X_t$$

$$J_{s,i} = v_s(X_{i+1}) \cdot X_{i+1} \quad \text{if } X_{i+1} \leq X_t$$

· Underflow zone ( $m \leq i \leq n - 1$ ):

$$J_{s,i} = \min \left( v_s(X_i) \cdot X_i, v_s(X_{i+1}) \cdot X_{i+1} \right) \quad (14)$$

This definition expresses that in the overflow zone, hindered settling occurs only if the solids concentration in layer  $i + 1$  exceeds a threshold value  $X_t$  [g/m<sup>3</sup>]. In the underflow zone, the settling regime is hindered settling no matter what the value of the solids concentration in layer  $i + 1$  is. The settling velocity is described by Equation (7).

#### 3.1 Numerical values used in the simulations

The values used for the model parameters, the design and operational variables, and the initial conditions are presented in Table 1 (all taken from Jeppsson and Diehl 1996). The resulting variation of the settling flux and the total solids flux in the underflow region (if the settling velocity from layer  $i$  is determined by  $X_i$ ) in function of the solids concentration is presented in Figure 4. The settling flux attains a maximum of 5314 g/h·m<sup>2</sup> at  $X$  equal to  $X_s^* = 2381$  g/m<sup>3</sup> and the total flux in the underflow region attains a maximum of 6365 g/h·m<sup>2</sup> at  $X$  equal to 2915 g/m<sup>3</sup>.

#### 3.2 Dynamic evolution of the concentration profile

The dynamic evolution of the concentration profile in the settler is plotted in Figure 5. The observed behavior starting from a uniform (zero) concentration can be explained on the basis of the model equations.

Table 1. Numerical values.

Model parameters		
$v_0$	145/24	[m/h]
$v'_0$	100/24	[m/h]
$X_{min}$	10	[g/m <sup>3</sup> ]
$r_p$	0.005	[m <sup>3</sup> /g]
$r_h$	0.00042	[m <sup>3</sup> /g]
$X_t$	3000	[g/m <sup>3</sup> ]
$n$	25	[-]
Design and operational variables		
$A$	500	[m <sup>2</sup> ]
Depth	4	[m]
Depth of the inlet	1.8	[m]
$Q_f$	450	[m <sup>3</sup> /h]
$Q_{un}$	200	[m <sup>3</sup> /h]
$Q_e$	250	[m <sup>3</sup> /h]
$X_f$	5200	[g/m <sup>3</sup> ]
Initial conditions		
$X_i$ ( $i = 1, \dots, n$ )	0	[g/m <sup>3</sup> ]

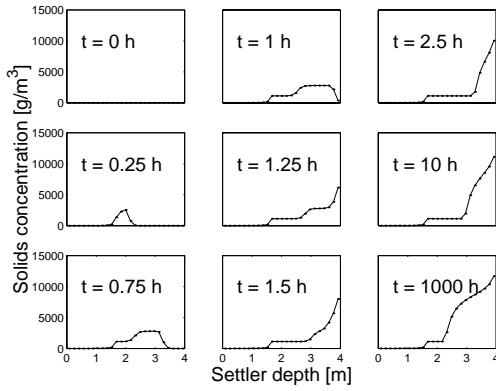


Fig. 5. Takács model: dynamic evolution of the concentration profile.

*Inlet layer.* The inlet layer concentration increases until the sum of the fluxes leaving the layer towards the underflow and the overflow zone equals the feed flux:

$$(q_{un} + q_{ov}) \cdot X_f = X_m \cdot (q_{un} + v_s(X_m)) + X_m \cdot q_{ov} - X_{m-1} \cdot v_s(X_{m-1}) \quad (15)$$

Because the steady state flux towards the effluent is negligible, this mass balance simplifies to

$$(q_{un} + q_{ov}) \cdot X_f = (q_{un} + v_s(X_m)) \cdot X_m \quad (16)$$

which can be solved for the inlet layer steady state concentration  $X_m$ .

*Overflow region.* The net settling flux into a layer  $i$  equals  $v_s(X_{i-1}) \cdot X_{i-1} - v_s(X_i) \cdot X_i$  and the net bulk flux into the layer is  $q_{ov} \cdot (X_{i+1} - X_i)$ . Equilibrium is reached when the negative effect of the settling flux compensates the positive bulk flux effect.

*Underflow region.* In the underflow zone, first a plateau of high concentration is formed that expands from the inlet layer in the downward direction. Meanwhile, the concentration in the inlet layer reaches its final value  $X_m$ , resulting in a flux towards the underflow region that is much smaller than the flux transported in the plateau of high concentration. Consequently, the plateau

is broken down (starting from the inlet layer), and layer after layer reaches the concentration  $X_m$  of the inlet layer.

The concentration in the bottom layer continues to increase because of a discontinuity in the flux definition: the flux towards the bottom layer is the sum of the bulk flux and the settling flux coming from layer  $n - 1$ , while the flux out of layer  $n$  only consists of a bulk flux. Steady state is reached when this outgoing bulk flux equals the flux entering the settler at the inlet level (the flux towards the effluent is neglected):

$$(q_{ov} + q_{un}) \cdot X_f = q_{un} \cdot X_n \quad (17)$$

Without a flux restraint, the concentration in the bottom layer would be the only one to increase beyond  $X_m$  (see Figure 3). However, the flux restraint (14) induces an increasing steady state concentration profile in the lower part of the underflow zone. In that zone the concentration turns out to depend only on  $X_n$  and  $q_{un}$ .

### 3.3 Effect of the loading characteristics on the steady state concentration profile

**3.3.1. Influent concentration.** The sensitivity of the steady state concentration profile for the influent concentration  $X_f$  is shown in Figure 6. For  $X_f$  equal to 3000, 4000, 4500 or 5000 g/m<sup>3</sup>, the dynamic evolution of the concentration profile is as described in Section 3.2. The inlet and bottom layer concentrations can be calculated using Equations (16) and (17) respectively: a higher value of  $X_f$  induces an increase of  $X_m$  and  $X_n$ .

The situation is different for  $X_f$  equal to 5300, 5500, 6000 or 7000 g/m<sup>3</sup>. The evolution of the profile for  $X_f$  equal to 5500 g/m<sup>3</sup> is presented in Figure 7. At first, the dynamic evolution is again as described in Section 3.2. However, as time proceeds the effect of the bottom layer discontinuity breaks through the inlet layer into the overflow zone. As a result, the flux restraint becomes active in the lower part of the overflow zone, inducing a plateau of constant (high) concentration.

**3.3.2. Influent flow rate.** Simulations have been performed for different values of the influent flow rate  $Q_f$ . The underflow flow rate  $Q_{un}$  is set equal to 200 m<sup>3</sup>/h while the effluent flow rate  $Q_e$  is computed from the balance  $Q_f = Q_e + Q_{un}$ .

Figure 8 illustrates that the effect of the influent flow rate  $Q_f$  on the steady state concentration profile is similar to the effect of the influent concentration  $X_f$ .

It can be concluded that a moderate increase of the influent solids flux (via  $X_f$  and/or  $Q_f$ ) induces a higher steady state concentration in the underflow, while the effluent concentration remains unaffected. However, a large influent flux increase overloads the settler, resulting in a non-negligible steady state effluent concentration.

### 3.4 Effect of the number of layers on the steady state concentration profile

The effect of the number of layers on the steady state concentration profile is demonstrated in Figure 9. As long as the number of layers in the underflow zone is equal to or larger than 11 (this number depends of course on all numerical values used during simulation), the obtained profile is as described in Section 3.2 for 25 layers. For each of the simulations, the concentrations in the inlet layer, the plateau of constant concentration and the bottom layer reach the same values, given by Equations (16) and (17). Furthermore, since the concentrations in the layers of the lower part of the underflow zone are functions of  $X_n$  and  $q_{un}$  only, they remain unaltered as well (albeit at different depth in the settler). If the number of layers below the inlet layer is less than 11, the effect of the discontinuity breaks through the inlet layer, and the concentration profile evolution is as illustrated in Figure 7.

Clearly, the Takács model is *inconsistent* with respect to the number of layers used during discretization. (When increasing the number of layers towards infinity, the flux restraint effect even disappears resulting in a profile as in Figure 3.) This inconsistency induces a serious parameter identification problem, as illustrated in Figure 10. In this example, the steady state concentration profile for  $n$  equal to 25 serves as data set, which is thereafter described by using the Takács model with  $n$  equal to 50. A reasonable fit is only possible after adjusting the parameter values (of Table 1) as follows:  $v_0 = 132.2/24$  m/h and  $v'_0 = 91.2/24$  m/h. Since the parameter values depend on the number of layers, it is senseless to assign a physical meaning to them.

#### 4. MODEL OF HAMILTON *ET AL.* (1992)

In an attempt to obtain a (more realistic) non-constant concentration profile in the underflow zone, restricting the settling flux after discretization of the continuity equation (1) has an unwanted side-effect: the model outputs strongly depend on the number of layers considered (see Section 3). An *alternative* refinement of the solid flux theory that creates a non-constant concentration profile in the underflow zone is the extension of the continuity equation with a (second order) *dispersion term* (Hamilton *et al.* 1992):

$$\frac{\partial X}{\partial t} + \frac{\partial J}{\partial z} - D \cdot \frac{\partial^2 X}{\partial z^2} = 0 \quad (18)$$

Discretization yields the following balances:

· Top layer (layer 1):

$$h \cdot \frac{dX_1}{dt} = q_{ov} \cdot X_2 - q_{ov} \cdot X_1 - J_{s,1} + D \cdot \frac{X_2 - X_1}{h} \quad (19)$$

·  $i$ -th layer in overflow zone ( $2 \leq i \leq m-1$ ):

$$h \cdot \frac{dX_i}{dt} = q_{ov} \cdot X_{i+1} - q_{ov} \cdot X_i + J_{s,i-1} - J_{s,i} + D \cdot \frac{X_{i+1} - X_i}{h} - D \cdot \frac{X_i - X_{i-1}}{h} \quad (20)$$

· Feed layer (layer  $m$ ):

$$h \cdot \frac{dX_m}{dt} = \frac{Q_f}{A} \cdot X_f - q_{ov} \cdot X_m - q_{un} \cdot X_m + J_{s,m-1} - J_{s,m} + D \cdot \frac{X_{m+1} - X_m}{h} - D \cdot \frac{X_m - X_{m-1}}{h} \quad (21)$$

·  $i$ -th layer in underflow zone ( $m+1 \leq i \leq n-1$ ):

$$h \cdot \frac{dX_i}{dt} = q_{un} \cdot X_{i-1} - q_{un} \cdot X_i + J_{s,i-1} - J_{s,i} + D \cdot \frac{X_{i+1} - X_i}{h} - D \cdot \frac{X_i - X_{i-1}}{h} \quad (22)$$

· Bottom layer (layer  $n$ ):

$$h \cdot \frac{dX_n}{dt} = q_{un} \cdot X_{n-1} - q_{un} \cdot X_n + J_{s,n-1} - D \cdot \frac{X_n - X_{n-1}}{h} \quad (23)$$

$D$  is the dispersion coefficient [ $\text{m}^2/\text{h}$ ]. The settling flux  $J_{s,i}$  between two adjacent layers  $i$  and  $i+1$  equals  $v_s(X_i) \cdot X_i$ . Hamilton *et al.* used the Vesilind equation to describe the settling velocity, while Watts *et al.* (1996) proposed to use the Takács settling velocity function in the Hamilton model. The right hand side of each balance equation explicitly depends on the layer height  $h$ . Therefore, the fluxes transported between layers depend on the number of layers used in the discretization step. As a result, the number of layers has only a *resolution effect* on the obtained concentration profile. This is illustrated in Figure 11, showing the steady state concentration profiles for three different  $n$ -values. (During simulation the Takács settling velocity function is used, and all parameter, initial, and operational values are taken from Table 1. For the dispersion coefficient  $D$  the value  $13/24$   $\text{m}^2/\text{h}$  is used.)

#### 5. CONCLUSIONS

Simulating the model of Takács *et al.* (1991) with different values of the feed concentration and the influent flow rate shows that at a low influent flux, the amount of solids transported to the effluent is negligible. A *moderate* increase of the influent solids flux induces a higher steady state concentration in the underflow, while the effluent concentration remains unaffected. However, a large influent flux increase overloads the settler, resulting in a non-negligible steady state effluent concentration (after breakthrough of the inlet layer). Simulations for different values of  $n$  reveals a major shortcoming of this model, namely, the inconsistency of the predictions with respect to the number of layers. This results in an identification problem: the parameter values need

adjustment each time the resolution of the model is changed. Therefore, restricting the solids flux after discretization is not the appropriate way to generate a (realistic) non-constant concentration profile in the settler. A better alternative is the extension of the (first order) continuity equation with a dispersion term, as proposed by Hamilton *et al.* (1992). In the Hamilton model, the number of layers used in the discretization step has only a *resolution effect* on the obtained concentration profiles.

#### ACKNOWLEDGMENTS

Author Liesbeth Verdickt is a research assistant with the Fund for Scientific Research-Flanders (FWO). Work supported in part by Projects OT/99/24 and IDO/00/008 of the Research Council of the Katholieke Universiteit Leuven and the Belgian Program on Interuniversity Poles of Attraction, initiated by the Belgian State, Prime Minister's Office for Science, Technology and Culture. The scientific responsibility is assumed by its authors.

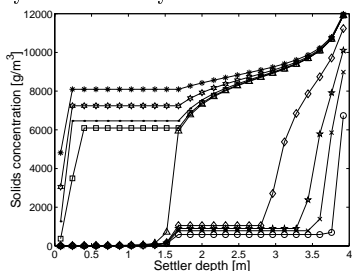


Fig. 6. Takács model: steady state concentration profiles for  $X_f = 3000$  (o), 4000 (x), 4500 (\*), 5000 (◇), 5300 (△), 5500 (□), 6000 (·), 7000 (hexagram) and 8000 (\*)  $\text{g/m}^3$  are presented.

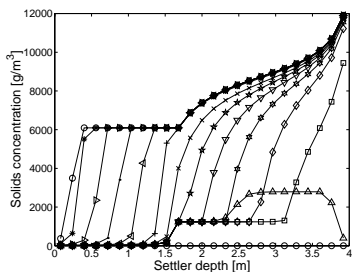


Fig. 7. Takács model: evolution of the concentration profile for  $X_f = 5500 \text{ g/m}^3$ , concentration profiles after 0 (o), 1 (△), 2 (□), 8 (◇), 16 (hexagram), 24 (▽), 32 (\*), 40 (x), 50 (+), 60 (◁), 70 (·), 80 (▷), 90 (\*) and 200 (o) hours.

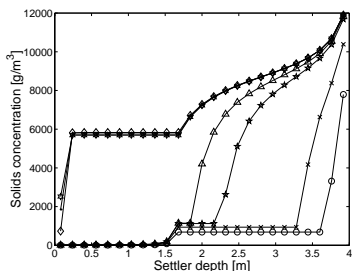


Fig. 8. Takács model: steady state concentration profiles for  $Q_f = 300$  (o), 400 (x), 450 (\*), 455 (△), 500 (◇), 600 (·) and 700 (hexagram)  $\text{m}^3/\text{h}$ .

#### 6. REFERENCES

- Dupont, R. and C. Dahl (1995). A one-dimensional model for a secondary settling tank including density current and short-circuiting. *Wat. Sci. Tech.* **31**(2), 215–224.
- Hamilton, J., R. Jain, P. Antoniou, S.A. Svoronos, B. Koopman and G. Lyberatos (1992). Modeling and pilot-scale experimental verification for predenitrification process. *J. Environ. Eng.-ASCE* **118**(1), 38–55.
- Jeppsson, U. and S. Diehl (1996). An evaluation of a dynamic model of the secondary clarifier. *Wat. Sci. Tech.* **34**(5-6), 19–26.
- Kynch, G.J. (1952). A theory of sedimentation. *Trans. Faraday Soc.* **48**, 166–176.
- Otterpohl, R. and M. Freund (1992). Dynamic models for clarifiers of activated sludge plants with dry and wet weather flows. *Wat. Sci. Tech.* **26**(5-6), 1391–1400.
- Queinnee, I. and D. Dochain (2001). Modelling and simulation of the steady-state of secondary settlers in wastewater treatment plants. *Wat. Sci. Tech.* **43**(7), 39–46.
- Takács, I., G.G. Patry and D. Nolasco (1991). A dynamic model of the clarification-thickening process. *Wat. Res.* **25**(10), 1263–1271.
- Watts, R.W., S.A. Svoronos and B. Koopman (1996). One-dimensional modeling of secondary clarifiers using a concentration and feed velocity-dependent dispersion coefficient. *Wat. Res.* **30**(9), 2112–2124.

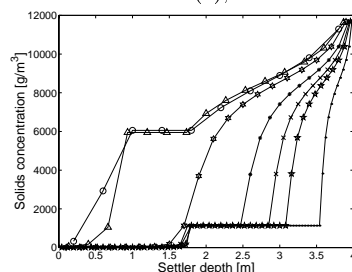


Fig. 9. Takács model: steady state concentration profile for  $n = 10$  (o), 15 (△), 20 (hexagram), 30 (\*), 40 (x), 50 (\*) and 100 (·).

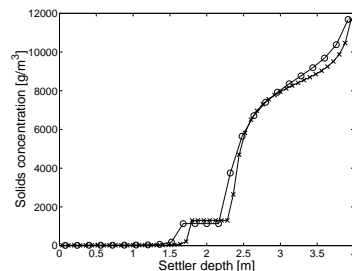


Fig. 10. Identification problem of the Takács model: simulation data for  $n = 25$  (o) and model with  $n = 50$  (x) fitted to these data.

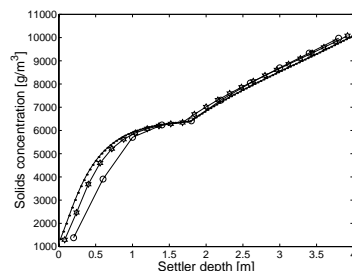


Fig. 11. Hamilton model: steady state profiles for  $n = 10$  (o), 25 (hexagram) and 100 (·).